INTERNATIONAL JOURNAL OF ADVANCE RESEARCH, IDEAS AND INNOVATIONS IN TECHNOLOGY

ISSN: 2454-132X
Impact factor: 4.295
(Volume 5, Issue 1)
Available online at: www.ijariit.com

Eddy Current Thermography for detection of edge defects in CrMo steel plate

Nakul Kumar
nakulkumar@bhel.in
National Institute of Technology, Tiruchirappalli, Tamil Nadu

Dr. R. Justin Joseyphus
rjustinj@nitt.edu
National Institute of Technology, Tiruchirappalli, Tamil Nadu

Dr. D. Sastikumar
sasti@nitt.edu
National Institute of Technology, Tiruchirappalli, Tamil Nadu

ABSTRACT

The present study considers the capabilities of Eddy current thermography for detection of Edge defects in metal plates. The focus is given on finding the location and dimensions of the defects available at the edge of metal plates. The study is performed on a slab of SA 387 Gr12(Killed steel), which has wide applications in power plants sector, oil and chemical Industry as pressure vessels, heat exchangers, industrial boilers, piping industry and in piping support structures. Small cracks in any of the components can lead to catastrophic failures which ask for the elimination of any stress concentrators at the time of manufacturing like Rolling. The study is performed on a sample with defects created at various angles. Similar cracks are also available in rails created because of Rolled Contact Fatigue. So the study will be useful for the detection of defects in rails also. ECT offers further prospects in extending into the area of automation and has specific advantages compared to conventional methods.

Keywords— *Eddy Current Thermography (ECT), Edge defects detection, A387GR12 inspection, Induction thermography*

1. INTRODUCTION

The Eddy Current Thermography (ECT) is an evolving contact-free, non-destructive method for crack testing of electroconductive materials and is a combination of two existing non-destructive testing methods, the depth sensitive eddy current testing and the fast and contact-free thermography [1,2]. It is a quick inspection method and can be used for detection and characterization of structural degradation and failures such as defect, fatigue, corrosion, and residual stress etc. This technique is able to detect hidden, subsurface defects even in complex geometry components. The parts to be tested are heated up by an inductively generated current flow and the temperature variation on the surface of the component is recorded with a thermographic camera. Cracks disturb the flow of the current in the component and thus change the temperature distribution as well, which can be detected thermographically with a high-resolution Infrared Camera (IR camera). This method has also a high application potential for closed cracks and cracks close under the surface where the dye penetrant inspection could not be used.

Various studies have been carried out so far for checking the suitability of ECT for surface and subsurface defects. Zainal Abidin [3] et al studied aluminium sample with angular slots for quantitative analysis of angular defects available on the surface. The author did experimental and simulation techniques for the identification of slot/defect angles and length. Yunze He [4] used a steel sample with perpendicular surface slots with varying lengths for detection of surface defects using phase analysis. It was shown that phase can eliminate the non-uniform heating and improve defect detectability comparing with the conventional thermograms in Eddy current pulsed thermography. Vrana [5] studied an analytical model for the calculation of the current distribution along with finite-element calculations for two different crack models (notch & slot). Netzelmann and Walle [6] discussed the application of induction thermography to inspect surface defects in forged components and ECT was found as an excellent alternative to MPT. Oswald-Tranta and Wally [7] explored the temperature distribution around the crack with different penetration depths using FEM modelling and experimental study. The results showed that in magnetic materials after a short heating period cracks are made visible by higher temperatures and in nonmagnetic materials by lower temperatures. Wally and Oswald [8] studied the influence of crack shape and geometry on the result of thermo-inductive crack detection. Thermal contrast, which is the temperature at crack divided by the temperature at the sample surface, was introduced to demonstrate the influence of different shapes on the thermal behaviour of cracks.

But less focus has been given towards detection of Edge defects and their quantification. Suixian Yang [9] et al did the simulation work for detectability of edge defects. The study was made with different defect sizes and defect detectability was ascertained. Also, it was found that thermal contrast decreases with increase in heating time so the heating time shall be kept least. Wilson et al

© 2019, www.IJARIIT.com All Rights Reserved

[10] did their work for imaging multiple cracks from rolling contact fatigue in the edges of rail heads for "Gauge Corner Cracking" (GCC) and "Head Checking (HC)". These edge cracks will cause a thermal distribution and same can be captured by the thermographic camera for defects detection. These studies were mainly focused on finding the detectability of defects. In this work, we will present the detection of the depth of defects and size of defects will be presented using the Eddy current thermography.

In the present study, we have examined simulated defects in GR12 plate of A387 (killed steel) which has wide applications in various industries. The experiment results for inspection of defects at various angles is discussed

2. THEORY OF EDDY CURRENT THERMOGRAPHY (ECT)

2.1 ASTM A387 or SA387 GR12 CL2 Cr-Mo Steel

The ASME SA387 standard covers the supply of weldable chrome molybdenum alloy steel plates for pressure vessels used in elevated temperature service. The added molybdenum and chromium provides excellent corrosion resistance and high-temperature resistance respectively [ASME BPVC.II.A]. For the present study, we have used A387GR12CL2 sample. As per ASME standard, it is engineered for use in elevated temperature service with applications in weldable pressure vessels and industrial boilers. In power plants, high thickness plates (thickness varying from 100 mm to 220 mm) are used for weldable pressure vessels. Lesser thickness plates are used in supporting structures for reheater, superheater etc. In the petrochemical industry inside the reactor, column, drums etc., it is used as internal support clips or brackets. The material benefits from added chromium which provides excellent corrosion and oxidation resistance making it ideal for sour service applications in the oil and gas industry. Tensile requirements as specified in ASME BPVC code as [11]:

Table 1: Mechanical properties of A387GR12

Chromium and Molybdenum content (according to the ASTM specification):		
Designation	**Nominal Chromium (Content (%))**	**Nominal Molybdenum (Content (%))**
A387 Grade 12	1.00%	0.50%
Tensile Requirements for Class 2 Plates:		
Designation	**Requirement**	**Grade12**
A387 Grade 12	Tensile strength, ksi [MPA]	65 to 85 [450 to 585]
	Yield strength, min, ksi [MPa]/(0.2% offset)	43 [310]
	Elongation in 8 in. [200mm], min %	18
	Elongation in 2 in. [50mm], min, %	22
	Reduction of the area, min %	——

2.2 Eddy Current Thermography

ECT can be used in line with other thermographic non-destructive evaluation (NDE) techniques such as sonic and laser spot thermography [1]. It involves heating of component/sample using induced currents using high power and high-frequency coil and observing the thermal response of the component using an infrared camera. Any surface or subsurface flaws will respond with a temperature gradient around itself.

2.2.1 Induction heating: Induction heating is a fast, efficient, precise, non-contact method for heating metals or electrically-conductive materials by means of electromagnetic induction. In this, a coil, suitably dimensioned and conducting high or medium frequency alternated current, is placed close to the metal parts to be heated, which induces eddy currents in the material. These eddy currents cause heating of the specimen, further, this heat is distributed to the nearby material by conduction. Heating occurs without any physical contact and very efficiently without any loss of energy. Induction heating is basically a combination of the following three principles:

(a) Electromagnetic induction
(b) Joule Heating
(c) Thermal conduction

(a) Electromagnetic Induction: Faraday's law of electromagnetic induction states that an emf is induced in a coil when magnetic flux through the coil changes with time and the direction of induced emf is given by Lenz law. That is:

$$\varepsilon = -d\Phi / dt \tag{1}$$

This flux change may be because of several reasons like relative movement between the coil and the primary coil (generating magnetic flux), or using a time-varying magnetic flux (Example induction heaters).

Eddy currents: When a bulk piece of the conductor is subjected to changing magnetic flux, induced currents are produced in them. However, their flow patterns resemble swirling eddies in water. This effect was discovered by physicist Foucault and these currents are called eddy currents or Foucault currents. The eddy currents intensity is given by:

$$i_{eddy} = i_{surface} * e^{-z\sqrt{(c\omega\mu\sigma)}} \tag{2}$$

Where, $i_{surface}$ is the current at the surface, z is the depth coordinate, c is a constant, σ is the conductivity of the material and μ is the magnetic permeability of the material.

© 2019, www.IJARIIT.com All Rights Reserved

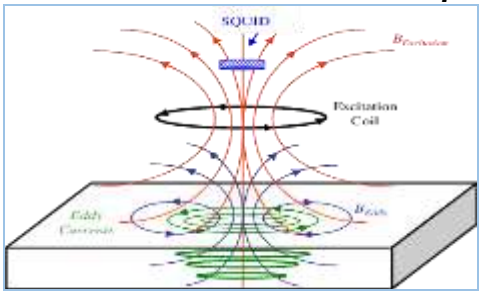

Fig. 1: Eddy currents generation

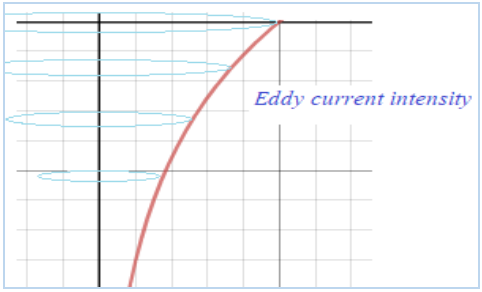

Fig. 2: Eddy current intensity

These eddy currents will cause the heating of the specimen. So the temperature distribution along the depth of the specimen will also be a similar profile caused by this eddy current heating. This temperature profile will be a signature profile for a particular material at a particular frequency and applied field for a given time. Presence of any flaw/crack/defect in the specimen will cause a disturbance to the flow of eddy currents and the temperature profile will change through the specimen and thus the signature temperature profile will be distorted. By analysing this temperature profile we will be able to detect the location and size of the defect as explained in the subsequent portion of this chapter.

(b) Joule Heating: Joule heating or resistance heating is the generation of heat by passing an electric current through a conductor. Joule's first law states that the heat generated by an electrical conductor is proportional to the product of its resistance, the square of the current and the time. So the eddy currents produced by a high energy coil encounter the resistance offered by the material of the sample/specimen which causes heating. Now with eddy currents, there are several other factors which shall be taken into consideration

The depth of penetration and skin depth: Eddy currents are more concentrated at the surface and decrease in intensity with distance below the surface of the metal. This effect is known as the "skin effect". The relation between them can be given as:

$$\delta = \sqrt{(2/(\omega * \mu_o * \mu_r * \sigma))} \quad (3)$$

Where, δ = standard depth of penetration (mm), ω = angular frequency (Hz), σ = conductivity (m/Ωmm^2), μ_o = permeability of free space and μ_r = Relative permeability.

Assuming conductivity and permeability to be constant for a selected material, a standard depth of penetration will be inversely proportional to the square root of applied frequency. Skin depth is sometimes used to design the thickness of current carrying wires.

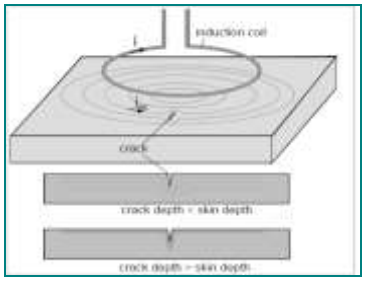

Fig. 3: Skin depth

(c) Thermal Conduction: The heat transfer by conduction and convection depend on various material characteristics like specific heat 'c', density 'ρ', thermal conductivity '*k*', thermal diffusivity 'α', temperature 'T'. Thermal inspection depends on differences in these material characteristics to establish a measurable and usually localized, temperature differential.

2.2.2 Infrared Thermography: As the name suggests, infrared thermography detects infrared energy emitted from an object, converts it to temperature, and displays image of temperature distribution. On the basis of the source to heat the specimen or the way to establish the heat blow thermography can be divided into two basic sections i.e. Active Thermography & Passive Thermography.

Now as in Active thermography an external stimulus is required to create the necessary gradient between defective and non-defective zone. Hence, on the basis of the heat source and the excitation mode, we can further categorize thermography. Source of stimulus can be:

- Optical Excitation
- Electromagnetic Excitation
- Mechanical Excitation

We will be using electromagnetic excitation in our experiment.

3. EXPERIMENTAL SETUP OF EDDY CURRENT THERMOGRAPHY

3.1 Specimen

A slab of SA387Gr12Cl2 (Cr-Mo steel) was used as a specimen for the study. Three samples with dimension 75mm x 60mm x 100 mm were cut from Cr-Mo steel plate. Now to make it similar with a real-time long edge defect, angular slots of dimension 7 ±

© 2019, www.IJARIIT.com All Rights Reserved

0.2 mm x 1.25 ± 0.25 mm are made throughout 60 mm width at angles of 30º, 60º and 90º with constant slot length and thickness in all 3 samples respectively using saw-cutting. Every specimen surface was painted with black paint to avoid reflection.

3.2 Induction heating system

The induction heating system used is an Indutech make Induction heater with a maximum power output of 1 kW. This energy is delivered to a copper coil and it produces a precisely controlled magnetic field over the workpiece. The system operates in the frequency range of 500 kHz.

3.2.1 Coil design: Figure 5 shows the coil used in the experiment.

- Material: Copper
- Geometry: Helical (with 4No of turns & constant base dia)
- ID: 42+-2 mm and OD: 50+-2 mm
- Copper tube Rad:4mm (used to make the coil)
- Coil lift off is 4.5 mm.

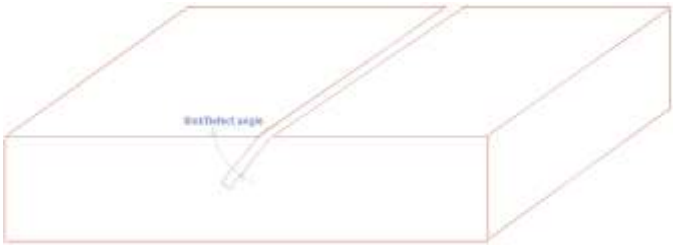

Fig. 4: Sample under the testing diagram

Fig. 5: Induction coil used in the experiment

3.2.2 IR Camera: The IR camera used for this experiment is FLIR SC 7500. The thermal profile detected by the camera sensor is converted to thermogram by using computer software. The camera used has an accuracy of 25mK and frame rate can go up to 380 Hz which determines the speed at which the camera can be operated. The camera records thermograms which can be evaluated and displayed using ALTAIR SOFTWARE. Origin 8 and MS Excel are used for plotting graphs.

3.3 Schematic Diagram

The schematic diagram for the process and the actual arrangement is shown in figure 6. The coil will induce eddy currents in the sample which will rush for the shortest closed path creating uneven heating around the defective region, and the same will be captured by IR camera and the image can be processed further.

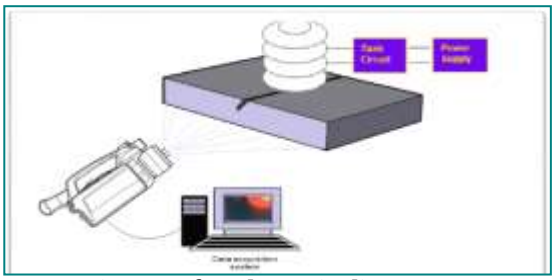

Fig. 6: Left: schematic diagram

Fig. 7: Left: schematic diagram

4. OBSERVATION AND ANALYSIS

4.1 Experiment observations and results

The experiment was performed with the coolant system for the coil and calibration of the IR camera. Induction Heater was set at full power of 1 kW so as to deliver a current of 400A. Power was tripped after 1s of heating and the sample was observed for a total of 10 sec. The excitation signal and the thermal response is similar to the one shown in figure 8.

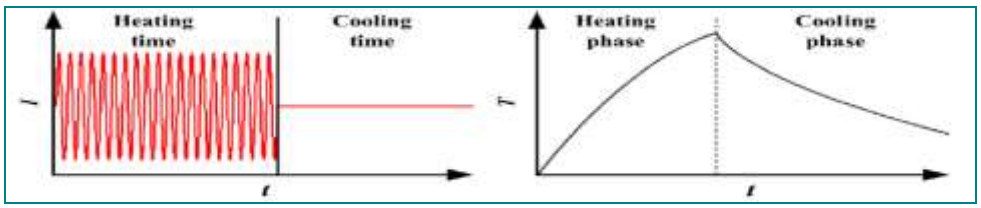

Fig. 8: Left: Excitation signal, Right: temperature response

Now various thermograms recorded for various angles are shown in figure 9. From the thermograms, it is clear that wherever the eddy currents are rushed/trapped more, the indication there is enough to give a strong thermo-visible indication for the defect. It is clear that for the lesser angle of trapment (A_t) or slot angle, defect angle like 30° or 45°, the temperature rise at the area indicated in figure 10 will be sudden because of concentrated eddy currents. When the slot angles are large like 60° and 90°, the trapped area has shifted to bottom as shown in figure 10 and the temperature indication of a defect will be strong in transmission mode.

© 2019, www.IJARIIT.com All Rights Reserved

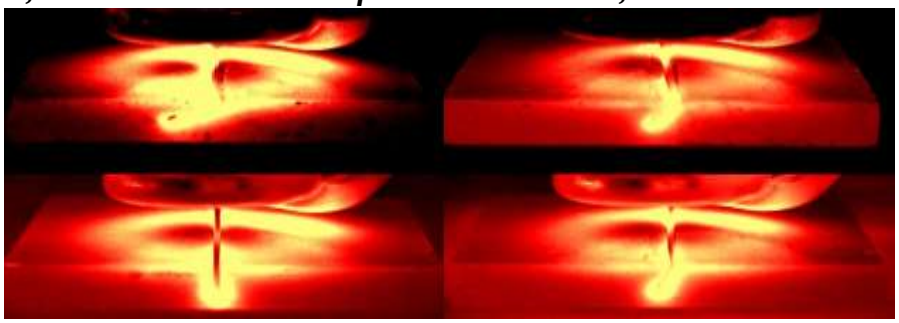

Fig. 9: Thermograms taken at 300ms: (Clockwise) 1: For 30° slot angle; 2: For 45° slot angle; 3: For 60° slot angle; For 90° slot angle

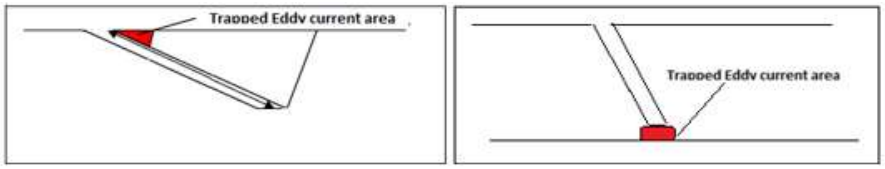

Fig. 10: Left: a Trapped area for less slot angle (30° and 45°); Right: a trapped area for more slot angle (60° and 90°)

During the cooling phase, the heat generated in the trapped area will be diffused to the neighbouring area which may cause a temperature rise in the neighbouring portion during the cooling phase also. Also, the heating zone will vary with the frequency and standard depth of penetration [Oswald and Wally]

Now an edge defect can be defined with dimensions a and b as in figure 11. In this, if a>b then it will act as a shallow defect and more eddy currents will be pushed under the defect and heating will be more there [Suixian Yang].

Now, here as we have created a defect throughout the width of the specimen, as shown in figure 12, so all eddy currents will divert under the defect and the defects deeper than Std. depth of penetration will also be visible from the side view. Same is clear from the thermograms shown in figure 9.

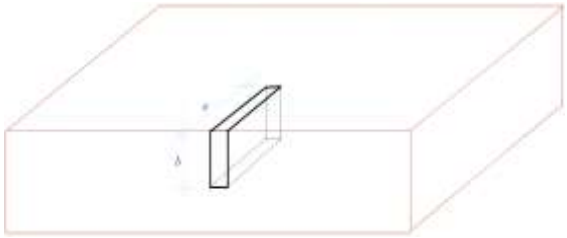

Fig. 11: Edge defect in a sample

Fig. 12: Throughout width defect created for the study

Temperature Profiles for side face

Now, if we draw a vertical line on the side face and take the temperature profile along this line in a defect-free sample, the profile will act as a reference for defect detection as already explained in section 2.2.1 (a). This is because the presence of a flaw will distort the path of eddy currents and thus the eddy current intensity will change in the specimen causing a change in this temperature profile.

We have drawn lines, as shown in figure 13, to take the temperature profiles. The temperature profile for a defect-free specimen will look like as shown in figure 14. The temperature data were taken at 0.70 seconds of heating. This temperature profile will be unique at a particular heating time and can be used as a reference for studying the specimen for defects for that particular slot angle.

Now to study further for edge defects, we will analyse the temperature profiles for all slot angles along the side face. For that we have drawn lines on the side face as shown in figure and temperature profile is recorded along these lines.

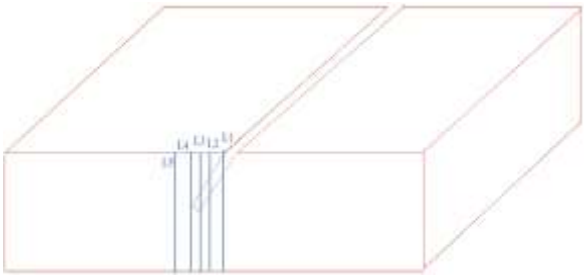

Fig. 13: Reference lines for analyzing temperature profile

Fig. 14: Temperature profile in defect free zone-reference profile

© 2019, www.IJARIIT.com All Rights Reserved

For 30°: We have drawn vertical lines in a region with a defect, as shown in below figure, and the temperature profile along these lines is analysed. Now with the presence of any defect in the specimen, the temperature profile will be distorted as the eddy currents path is disturbed which will give us an indication about the presence of a defect.

To study the same, we have drawn 5 lines in the defective zone for 30º slot angle as L1, L2, L3, L4, L5 at a distance of 0mm, 1.5mm, 3mm, 5mm, 7mm from the tip of the edge respectively. L0 denotes the vertical temperature profile in a defect-free zone. Same are shown in figure 13.

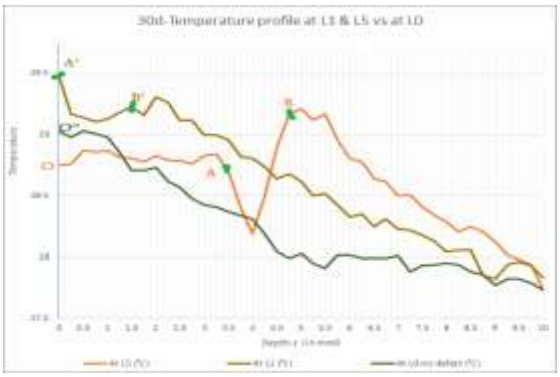

Fig. 15: Temperature profile along Line L1 & L5 against L0 -30° slot angle (left)

Fig. 16: Temperature profile along Line L2, L3 & L4 against L0 -30° slot angle (right)

In figure 15, L0 indicates the temperature profile for a defect-free zone which denotes the decrease of temperature with depth. Now, this profile is a reference profile for us at a particular heating time for the experimental setup

Above figure 15 indicates the temperature profile at line L5 for a sample with the angular defect at an angle of 30º. From this, it is clear that the temperature will be more in a zone with trapped eddy current than that of temperature in defect-free zone because of the rushing of eddy currents in this zone as shown in figure 10, Also, the heat will diffuse from the tip to the neighbouring area, thus the temperature slope is comparative less in a trapped zone as depicted by a curve from O to A. At point A, we see a sudden drop in temperature which is uneven as compared to the profile of a defect-free zone. This indicates the presence of a zone of different material properties i.e. a crack in this case and it marks the beginning of the crack opening. Subsequently there is a sudden increase in temperature to point B which marks the other end of the crack opening. So the abscissa distance between A and B defines the width of the crack and distance from O to A will indicate the depth of the defect from the surface.

Similarly for line L1, as the line is drawn from the tip, the temperature at the surface is much more than the temperature in a defect-free zone. Suddenly we see an immediate drop in temperature at point A' which indicate the beginning of a crack. Further, there is again temperature increase to point B' which indicates the other end of the defect. So the distance between A' & B' denotes the depth/width of the defect.

Defect starting and endpoint can also be found similarly along line L2, L3 & L4.

At surface that is at the start point of curves (at points, O' & O'') temperature for L2>L3>L4. This is because of more trapped eddy currents as the slot angle is pretty steep and nearer the point to the tip more is the current density and thus the temperature.

For 60º: We have drawn 4 lines in the defective zone for 60º slot angle as L1, L2, L3, L4 at a distance of 0mm, 1.5mm, 3mm, 5mm from the tip of the edge respectively. L0 denotes the vertical temperature profile in a defect-free zone

It is obvious from the figure 17 that, in contrary to the case of 30º slot angle in figure 15, here it can be noted from below graph that the difference is not much between the temperatures at surface that is at starting point of profile for L1, L2 & L0 at point O. This may be because of lesser trapped eddy currents in the zone due to slant slot angle.

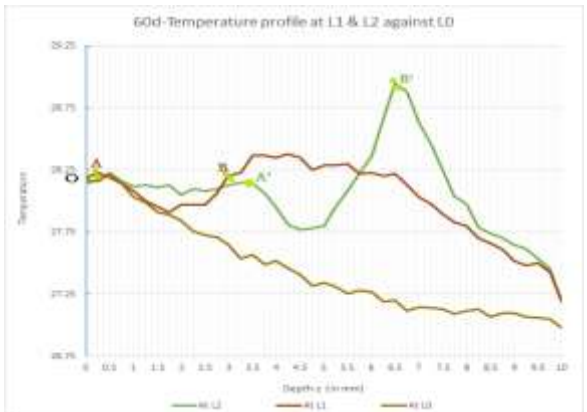

Fig. 17: Temperature profile along Line L1 and L2 against L0 -60° slot angle (Left)

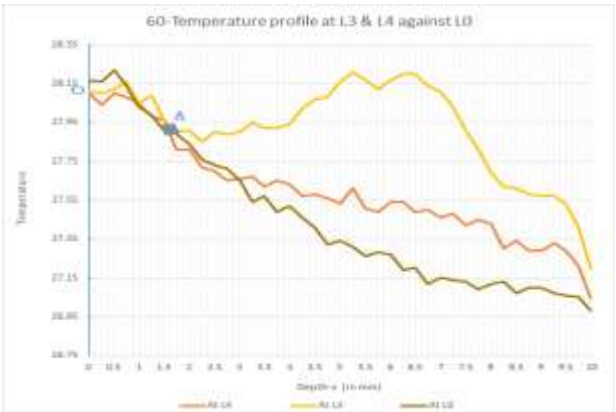

Fig. 18: Temperature profile along Line L3 and L4 against L0- 60° slot angle (Right)

© 2019, www.IJARIIT.com All Rights Reserved

Here in figure 18, the temperature profile is almost the same up to point A. After point A, for L3, the temperature rise is very gradual and not sudden. This depicts that the line L3 doesn't cross the defect but is in the vicinity of the same and indicates the presence of a nearby defect. Now as temperature decrease initially and then increases later at a certain depth which indicates the presence of a nearby angular/horizontal defect.

For line L4, profile traced is similar to L0 profile but with a little less slope and more temperature, which can be because of diffusion of heat from a nearby trapped heat zone as shown in below figure 19.

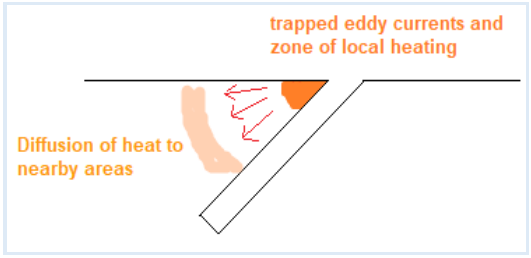

Fig. 19: Diffusion of heating from localized heating zone to neighbouring area

For 90º: In contrary to the general temperature profile for a no-defect sample, L1 indicates a very less temperature at the surface which indicates a defect which is open to surface i.e. an edge defect. Temperature is increasing gradually with depth and reaches a maximum at a point which indicates the defect shall be a vertical defect up to a depth measured by abscissa of OA. For L2 & L3, the temperature profile is the same up to point Z followed by a gradual increase in temperature. This indicates the line is in the vicinity of a defect.

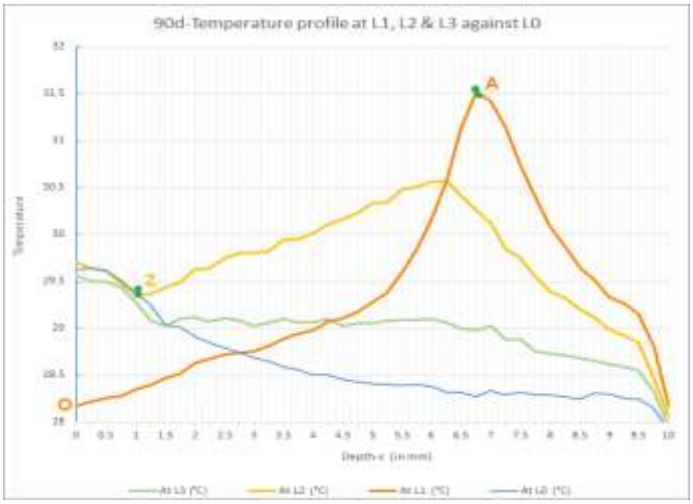

Fig. 20: Temperature profile along Line L1, L2 & L3 against L0 - 90° slot angle

With the above data, we have made a table comparing the theoretical values and the experimental values of defect depth and height.

Table 2: Geometrical values vs experimental values of defect depth and defect height

Slot angle (degrees)	Location (line drawn for taking temp profile)	The distance of the line from defect tip (mm)	Geometrical value		Experimental value	
			The depth of defect from the surface (mm)	Height/width of defect (mm)	The depth of defect from the surface (mm)	Height/width of defect (mm)
30	L1	0.00	0.00	1.44	0.00	1.50
	L2	1.50	0.00	1.25	1.00	1.25
	L3	3.00	0.00	1.25	1.50	1.25
	L4	5.00	0.00	1.25	2.50	1.25
	L5	7.00	0.00	1.25	3.50	1.25
60	L1	0.00	0.00	2.50	0.25	2.75
	L2	1.50	0.00	1.25	3.75	2.75
	L3	3.00	No defect	No defect	-	-
	L4	5.00	No defect	No defect	-	-
90	L1	0.00		7.00	0.00	6.75
	L2	1.50	No defect	No defect	-	-
	L3	3.00	No defect	No defect	-	-

The table shows that the experimental values for defect depth and height are same to the theoretical values with a tolerance of 0.25mm which can be rectified by various image processing tools or using Phase analysis [4].

© 2019, www.IJARIIT.com All Rights Reserved

5. AUTOMATED-ECT

The automation possibilities of the different steps involved in an inspection make thermography an interesting alternative to manual inspection methods such as fluorescent penetration inspection (FPI) [12]. Netzelmann and Walle [6,13] discussed the automation of ECT using robotics for the handling of component and induction coils and also about the standardization of induction thermography and inspection of rails and train wheels performed for surface defects. However, automated movements of components or induction coils are being discussed for the ease of inspection. But it is more interesting to even explore the area of final decision making after automated inspection. A reference can be set similar to GO/NO-GO gauges so as to set up an Accept-Reject criterion. It basically asks for a reference sample/table/charts similar to other NDE techniques.

Specific to a product or a production line, with our past experience and with the help of other NDE techniques, a Reference/Trueflaw sample-set can be prepared. This Trueflaw sample-set shall have the possible/desired defects for that production line. Now, this Trueflaw-sample-set sets the limit of Accept-Reject criterion for our production line. Eddy current thermography study can be performed for this sample set. With the help of these thermograms (as available in the previous section of this paper) temperature graphs, amplitude & phase images can be generated. From the amplitude and phase images [4], the Accept-Reject criterion can be set for our production line. With the available advancement in software development and image processing, the maximum readings available with us can be linked/fed in the image processing software of our thermal camera. For all the components produced in the production line, for which the thermal readings as measured by the thermal camera are higher than the set limits, those components can be rejected or marked for further evaluation. This way, the whole production line including inspection decision can also be automated.

Especially for Edge defects the thermal profiles for defect-free item can be recorded and set as a reference for decision making can be clubbed with the production line with the help of logical-circuits. Wherever it detects any deviation, more than the tolerance limit, from the thermal profile the area/zone can be marked or straightaway Accept/Reject decision can be taken automatically.

6. CONCLUSION AND OUTLOOK

The experimental model presented here gives a good understanding of the thermographic inspection of edge cracks in-service components. ECT proves to be an effective technique for inspection of edge defects. Materials are easy to inspect and defect locations and dimensions can be measured with considerable accuracy. Materials are easy to inspect and with the help of robotics, it can be automated easily for suiting to production lines.

With the quickness of visible inspection and accuracy, ECT is an emerging technique which can be explored to be a credible alternative to various other conventional NDE methods. With the use of automation, the inspection time can be reduced to a few seconds at low inspection costs.

7. REFERENCES

[1] G. Zenzinger, J. Bamberg, W. Satzger and V. Carl. Thermographic crack detection by eddy current excitation, NDT&E 22 (2007) 101.
[2] Gui Yun Tian, Yunze He et al Eddy Current Pulsed Thermography with different excitation configurations for metallic material and Defect characterization, Sensors 16 (2016) 843.
[3] Ilham Zainal Abidin, Gui Yun Tian, John Wilson, Suixian Yang, Darryl Almond. Quantitative evaluation of angular defects by pulsed eddy current thermography. NDT&E Intl. 43-2010)- 543.
[4] Yunze He, GuiYun Tian, Mengchun Pan and Dixiang Chen. Eddy current pulsed phase thermography and feature extraction, Applied Physics Letters 103 (2013) 84104.
[5] J. Vrana, M. Goldammer, J. Baumann, M. Rothenfusser, and W. Arnold. Mechanisms and Models for Crack Detection with Induction Thermography. in AIP Conference Proceedings · February 2008
[6] U. Netzelmann and Günter Walle. Induction Thermography as a Tool for Reliable Detection of Surface Defects in Forged Components. 17th World Conference on Nondestructive Testing, 25-28 Oct 2008, Shanghai, China.
[7] Beate Oswald-Tranta, Gernot Wally. Thermo-Inductive Surface Crack Detection in Metallic Materials. ECNDT 2006-We.3.8.3
[8] Gernot Wally, Beate Oswald-Tranta. The Influence of Crack Shapes and Geometries on the Result of the Thermo-Inductive Crack Detection. Thermosense XXIX edition
[9] Suixian Yang, Gui Yun Tian, Ilham Zainal Abidin, John Wilson. Simulation of Edge Cracks Using Pulsed Eddy Current Stimulated thermography. Journal of Dynamic Systems Measurement and Control Vol 133, Jan-2011.
[10] John Wilson, GuiyunTian, IlhamMukriz, Darryl Almond. PEC thermography for imaging multiple cracks from rolling contact fatigue. NDT&E International44(2011)505–512
[11] Aesteiron Steels LLP, http://www.aesteiron.in/, retrieved on Dec 2018.
[12] M. Goldammer, H. Mooshofer, M. Rothenfusser, J. Bass, and J. Vrana. Automated induction thermography of generator components, AIP Conference Proceedings 1211 (2010) 451.
[13] U. Netzelmann, G. Walle, S. Lugin, A. Ehlen, S. Bessert and B. Valeske. Induction thermography: principle, applications and first steps towards standardization, Quant. IR Therm. J. 13 (2016) 170.

© 2019, www.IJARIIT.com All Rights Reserved